

Comparison Between Experimental and Theoretical Model of Highly-Efficient GaInP/Si Tandem Solar Cells

Rached Ganouni, Mourad Talbi and Hatem Ezzaouia
Center of Research and Technologies of Energy of Borj Cedria, Tunis, Tunisia

Abstract: Si based tandem solar cells speak to a contrasting option to conventional compound III-V multi-junction cells as a promising approach to accomplish high efficiencies. In this study, we compare between an experimental model of a novel 4-terminal tandem cell design with a Back-Junction Back-Contacted (BJBC) c-Si and a theoretical model of a new structure of tandem solar cell based on c-Si using MATLAB code. The result obtained shows that we can arrived to the same efficiency $\eta = 28\%$ with the both of model but with less cost and problems of physics coherence in our model.

Key words: Tandem, solar cell, c-Si, efficiency $\eta = 28\%$, model, promising

INTRODUCTION

Multijunction solar cells based on III-V semiconductors are promising as a good innovation for next generation high-efficiency solar cells (Cotal *et al.*, 2009). Given that Si is the most popular semiconductor materials in the practical photovoltaic, multi-junction cells should be fabricated on Si. However, III-V-on-Si multi-junction cells cannot be easily fabricated for many reasons as an example the difference in lattice constant and thermal expansion coefficients between III-V materials and Si (Green *et al.*, 2005). As result we think about a new architecture between III-V materials and Si.

In this study, we will develop a comparison between experimental model of a novel 4-terminal tandem cell design with a Back-Junction Back-Contacted (BJBC) c-Si (Essig *et al.*, 2015) and a new provision of tandem solar cell by a model that will describe an innovation in the field of photovoltaic and avoiding the problems already announced. This model is based on a rigorous theoretical calculation using MATLAB code (including optical and electrical modules). This study focus on the design of a two junction GaInP/c-Si solar cell, under the standard AM1.5 solar spectrum including the design of separation of cells in order to avoid the problem of mismatch between c-Si and III-V materials. Finally, we determined the reflectance, current density and efficiency of this new model and compare to the experimental model.

MATERIALS AND METHODS

Theoretical approach

Introduction of model: In this study, we propose a new model of GaInP/c-Si tandem solar cell based on parabolic

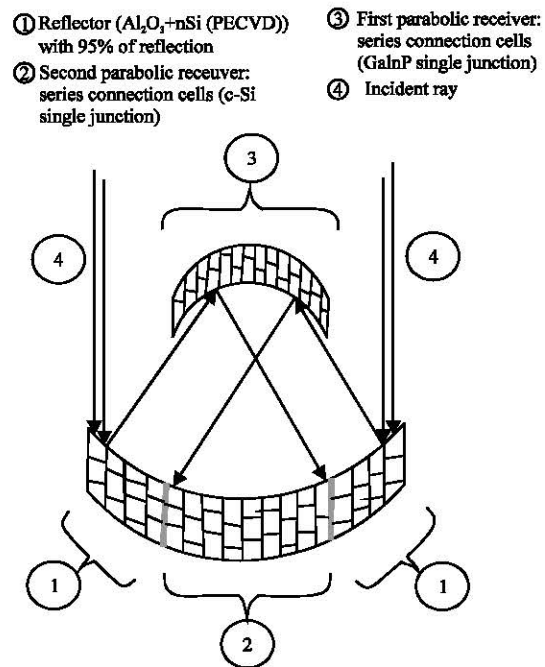


Fig. 1: New model of tandem solar cells with parabolic trough concentrator (In French: concentrateur cylindro-parabolique)

trough concentrator. This model is illustrated in Fig. 1. As shown in Fig. 1, this model is constitutes of two parabolic systems. The first parabolic system includes a single region 2 located between two regions 1 having the same surface and each of them contains a reflector with 95% of reflexion (composed by $\text{Al}_2\text{O}_3+\text{nSi}$ (PECVD)). The region 2 contains a c-Si single junction solar cells connected in series. Each of these solar cells is modeled in Fig. 2. The

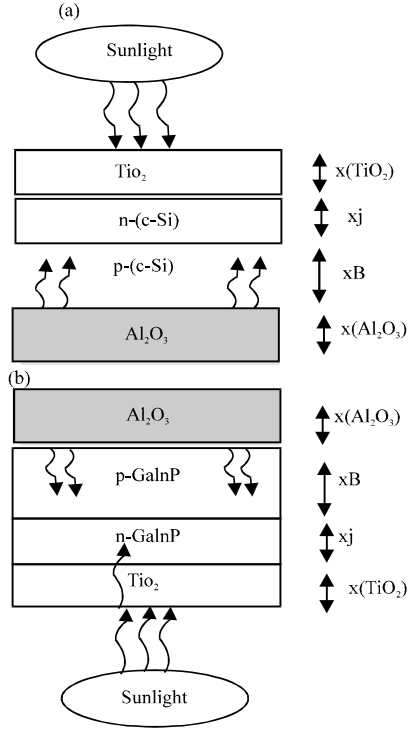


Fig. 2: Composition of GaInP and Si solar cells: a) c-Si single junction cell and b) GaInP single junction cell

second parabolic system contains a GaInP single junction solar cells connected in series, each of these solar cells is modeled in Fig. 2.

Each of GaInP or c-Si cell is composed by absorber layer TiO₂, p-n junction and reflective layer Al₂O₃ (Fig. 2 (a and b) c-Si single junction solar cells and (b) GaInP single junction solar cells). The solar radiation arriving on both regions of the first parabola will undergo a total reflection to arrive at the second parabola. A large part of the spectrum will be absorbed by the cell of large gap GaInP, the rest is reflected from this cell to be absorbed by the cell c-Si. Light is reflected by the back surface of c-Si and we win the most of energy. The study of our structure is based on the calculation of three fundamental terms. Reflectance R, external quantum efficiency QE and current density J.

The optical demonstrating proposed in this study depends on the transfer matrix formalism. It permits calculation of the incident optical spectrum on each subcell from the solar cell spectrum. Each layer of the multi-junction is depicted by a transfer matrix M which is characterized by:

$$M = \begin{pmatrix} m_{11} & m_{12} \\ m_{21} & m_{22} \end{pmatrix} = \begin{pmatrix} \cos(\delta_j) & \frac{i \sin(\delta_j)}{N_j} \\ i N_j \sin(\delta_j) & \cos(\delta_j) \end{pmatrix} \quad (1)$$

$$\delta_j = \frac{2\pi N_j}{\lambda} d_j; \quad N_j = n_j(\lambda) + i k_j(\lambda)$$

where $n_j(\lambda)$, $k_j(\lambda)$ and d_j are the refraction, extinction index and the thickness of the layer, respectively. λ is the wavelength. The reflectance coefficient R (Yamaguchi, 2003) of the layer is then given by:

$$R = |r|^2 = \frac{n_0 m_{11} + n_s m_{12} - m_{21} + n_s m_{22}}{n_0 m_{11} + n_s m_{12} - m_{21} + n_s m_{22}} \quad (2)$$

where n_0 is the superstrate refractive index and n_s is the substrate refractive index. The $m_{j,n}$ coefficients refer to the matrix transfer elements. Thus, it is possible to search the appropriate thickness of layer to calculate QE and J.

Multi-junction cells act like homojunction cells in series and their open circuit voltage is the aggregate of the voltages of the subcells while their short circuit is that of the subcell with the littlest current. Thus, the execution of a multi-junction cell can be acquired from the execution of each subcell assessed freely. For each subcell, the load current density J is given by the superposition of two diode currents and the photo-generated current (Guijiang *et al.*, 2010):

$$J = J_{ph} - J_{01} (e^{qV/kT} - 1) - J_{02} (e^{qV/2kT} - 1) \quad (3)$$

Where:

- J_{ph} = The photocurrent density
- J_{01} = The ideal dark saturation current component
- J_{02} = The space charge non-ideal dark saturation current component
- k = The Boltzmann constant
- q = The electron charge
- T = The temperature ($T = 25^\circ\text{C}$) and V the voltage

The photocurrent density is given by the aggregate of the photocurrents created in the emitter, the base and the depleted region of the cell. Also, the dark current density is given by the entirety of the dark currents produced in the emitter, the base and the depleted region of the cell (Guijiang *et al.*, 2010), we have:

$$J_{ph} = J_{emitter} + J_{base} + J_{depleted} \quad (4)$$

This model incorporates optical and electrical modules with the optical modules permitting the examination of the appropriate thickness for each layer (x_j , x_B , $x(\text{TiO}_2)$ and $x(\text{Al}_2\text{O}_3)$) of GaInP and c-Si. At that point, the electrical model computes the photocurrents in the space charge region, the emitter and the base for every junction.

Solar cell structure and parameters: The wavelength-dependent reflectance coefficient of GaInP and c-Si is based on the research of fitting curves of extinction $n_j(\lambda)$ and refractive $k_j(\lambda)$ index. The fit for this curves (Fahrenbruch *et al.*, 1983; Wurfel, 2005; Luque and Hegedus, 2011) is given by:

$$\begin{aligned}
 *n(\lambda) [\text{GaInP}] &= 3.26 + \frac{8916.49}{4(\lambda-408)^2} + 21609 \\
 *k(\lambda) [\text{GaInP}] &= -0.0169 \frac{34520}{4(\lambda-334.2)} + 15672 \\
 *n(\lambda) [\text{c-Si}] &= 3.31 + 9.46 * \exp(-0.0042 * \lambda) \\
 *k(\lambda) [\text{c-Si}] &= -0.074 + 263.54 * \exp(-0.0136 * \lambda) \\
 *n(\lambda) [\text{TiO}_2] &= 2.59 + 1.71 e \left\{ 1 - \left[\frac{(a-325.98)}{38.99} e^{-\frac{-(\lambda-325.93)}{38.99}} \right] \right\} \\
 *k(\lambda) [\text{TiO}_2] &= 1.167 - 1.162 \left(\coth(\lambda-336.26) - \frac{1}{\lambda-336.26} \right) \\
 *n(\lambda) [\text{Al}_2\text{O}_3]^{[10]} &= 2.29623 + \frac{0.17963}{1 + e^{\frac{(\lambda-532.1490)}{35.08544}}} \\
 *k(\lambda) [\text{Al}_2\text{O}_3] &= 0
 \end{aligned}$$

The incident photon flux F for AM1.5 spectrum is taken by a fitting curve:

$$F = \frac{E_{cl}(\lambda)}{hc / \lambda} \quad (5)$$

$$\begin{aligned}
 E_{cl}(\lambda) &= 0.06977 + 7.065 \\
 &\left[1 - e^{\frac{-(\lambda-0.26058)}{0.15994}} \right]^{2.28411} e^{\frac{-(\lambda-0.26058)}{0.2285}} \quad (6)
 \end{aligned}$$

For $300 \text{ nm} < \lambda < 1400 \text{ nm}$. Where $E_{cl}(\lambda)$ (KW/m² μm) the illumination, h Planck constant, c velocity of light. The incorporated ASTM sub-committee G3.09 AM1.5 solar spectral irradiance has been made to adjust to the estimation of the solar constant acknowledged by the space community which is 694 W/m².

The diverse factors of c-Si and GaInP are characterized in Table 1 and 2. The absorption coefficient of GaInP can be fitted by:

$$\alpha (\text{GaInP}) = 5.5 \sqrt{E-E_g} + 1.5 \sqrt{E-E_g-1} \quad (7)$$

The absorption coefficient of c-Si can be fitted by:

$$\alpha (\text{c-Si}) = 0.0312 + 0.00114 * \exp(2.88 * E) \quad (8)$$

Table 1: Values for the parameters of c-Si^[12] and GaInP^[13] used in the model calculation

Parameters	c-Si	GaInP
Band gap $E_g(\text{eV})$	1.1	1.86
The electron surface recombination velocity $S_n(\text{cm/sec})$	10^2	$1.7 \cdot 10^6$
The hole surface recombination velocity $S_p(\text{cm/sec})$	10^3	10^4
Electron diffusion length $L_n(\mu\text{m})$	646	3
Hole diffusion length $L_p(\mu\text{m})$	1.18	0.5
Electron diffusion coefficient $D_n(\text{cm}^2/\text{sec})$	41.8	100
Hole diffusion coefficient $D_p(\text{cm}^2/\text{sec})$	1.39	5

Table 2: Values for the parameters c-Si^[12] and GaInP^[14] used in the model

Parameters	c-Si	GaInP
Concentration of acceptors $N_A(\text{cm}^{-3})$	$2 * 10^{15}$	10^{13}
Concentration of donors $N_D(\text{cm}^{-3})$	$1.25 * 10^{17}$	10^{17}
Intrinsic carrier concentration (cm^{-3})	$4.29 * 10^{10}$	$1.9 \cdot 10^{12}$
Permittivity	11.6	11.8

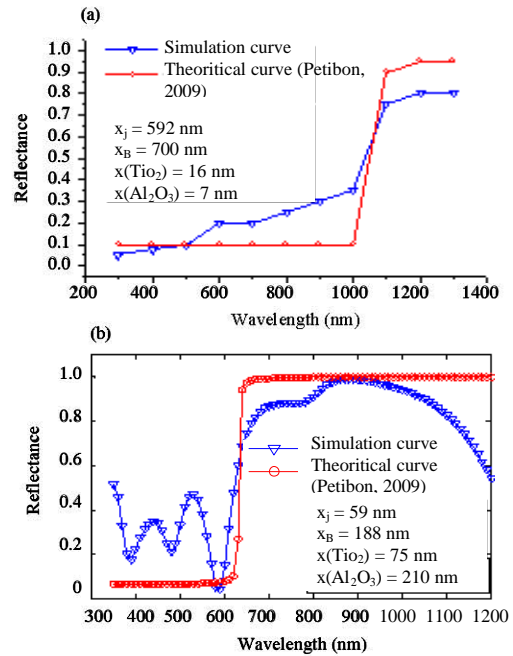


Fig. 3: The reflectance curve of: a) c-Si and (b) GaInP

where, E is the photon energy and E_g is the fundamental band gap, both in eV and α in 1/μm.

Simulation and results: In this study, we have varied the thickness of each layer in order to have from MATLAB simulation, a suitable reflectance curve for each cell and this by referring to the ideal theoretical curve. In Fig. 3a and b are illustrated the reflectance curves obtained from MATLAB simulation and from the theoretical formula given as follow (Petibon, 2009):

$$E_g (\text{eV}) = \frac{1.24}{\lambda_g (\mu\text{m})} \quad (9)$$

where $E_g(\text{eV})$ and $\lambda_g(\mu\text{m})$ are band gap energy and wavelength, respectively. This formula explains the

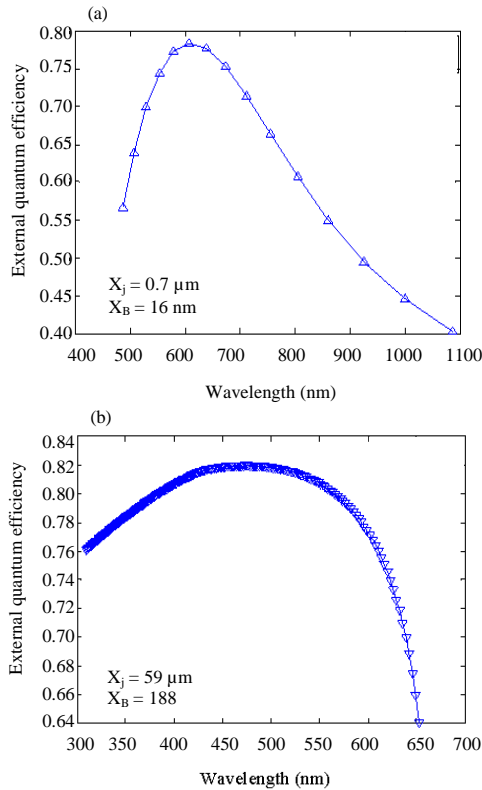


Fig. 4: The external quantum efficiency of c-Si and GaInP

variation of E_g (eV) vs. λ_g (μm) (Red curve in Fig. 3a and b. For c-Si, E_g (eV) = 1.1, this mean that λ_g (μm) = 1.12. This result explain that c-Si absorb for $\lambda < 1127$ nm (Reflectance = 0) and reflect all light for $\lambda > 1127$ nm ($R \approx 1$). For GaInP, E_g (eV) = 1.86, this mean that λ_g (μm) = 0.66. This result explain that GaInP absorb for $\lambda < 660$ nm (Reflectance = 0) and reflect all light for $\lambda > 660$ nm ($R \approx 1$).

The simulation curve give for c-Si $x_j = 592$ nm, $x_b = 750$ nm, $x(\text{Tl}_2\text{O}_2) = 16$ nm, $x(\text{Al}_2\text{O}_2) = 7$ nm and for GaInP $x_j = 59$ nm, $x_b = 188$ nm, $x(\text{Tl}_2\text{O}_2) = 75$ nm, $x(\text{Al}_2\text{O}_2) = 210$ nm.

Figure 3 demonstrates the ideal intelligibility amongst theoretical and simulation proposed, along this line the absorption of c-Si is important in the scope of wavelength 300-1127 nm whereas for GaInP is in the scope of 300-650 nm. This outcome is critical to the following work, along this lines we can with the estimations of thickness x_j and x_b represent the curve of external quantum efficiency and density of current. Figure 4 and 5 demonstrate the aggregate total external quantum efficiencies QE and the integrated photocurrent density J_{ph} of the two cells computed from Eq. 4. The external quantum efficiency is a component of wavelength and the photocurrent density J_{ph} is acquired from the integral of the product of quantum efficiencies (We can use too this rule:

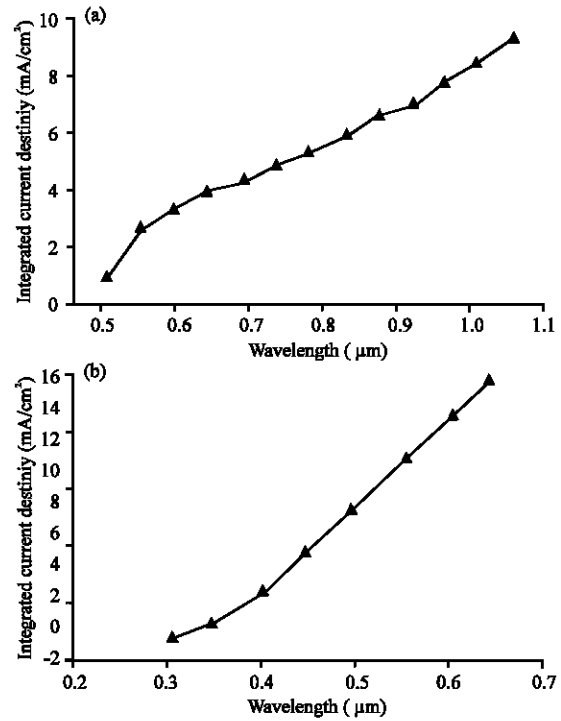


Fig. 5: Integrated photocurrent density of c-Si and GaInP: a) Si-monocrystallin and b) GaInP the high bandgap cell

$$J_{ph} = \sum_{i=1}^n (J_{ph}(\lambda_i)) \quad (10)$$

Figure 5 integrated photocurrent density of c-Si and GaInP. The high band gap cell GaInP generates a photo current density of 16 mA/cm², the low bandgap cell c-Si generates only 9.2 mA/cm². Figure 6 show I-V characteristics for each subcell c-Si and GaInP.

For the case of a cell with the new structure without tunnel junction and with a serie connection between sub-cells, J_{sc} , V_{oc} , FF and conversion efficiency η were determined for each of the junctions. Figure 7 shows the J-V curves for each of the sub-cells and the tandem cell in the new model. These curves for the series-connection cells was made using the equivalent circuit for 2 cells in series, $J_{ph}(\text{GaInP}) = J_{ph}(\text{GaAs}) = J_{ph}$ (Series-connection model) = 9.2 mA/cm². The resultant J-V and is shown in Fig. 7. These results are summarized in Table 3. For the proposed tandem solar cell $J_{sc} = 9.2$ mA/cm², $V_{oc} = 2.4$ V, FF = 0.94 and $\eta = 28\%$. This is expected high conversion efficiency under the AM1.5 solar spectrum, comparable to current technology two junction solar cells and there for et he GaInP/c-Si solar cell studied here is an attractive alternative for high efficiency solar energy conversion.

Experimental model: The theoretical model is compared to an experimental model based on a novel 4-terminal tandem cell design with a Back-Junction

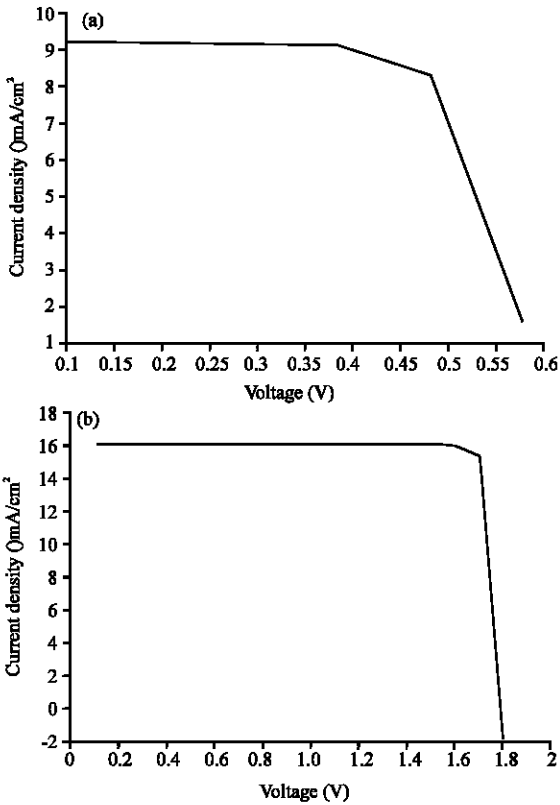


Fig. 6: I-V characteristics of GaInP and c-Si under AM1.5

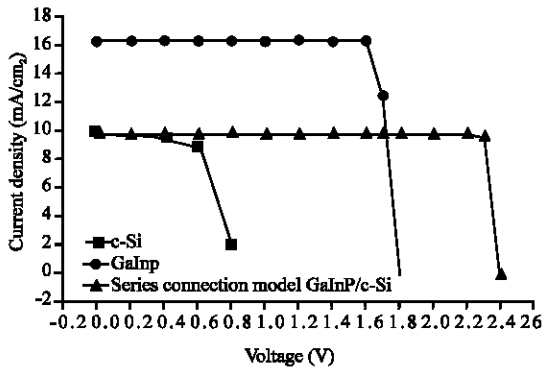


Fig. 7: I-V characteristics of the series-connections between GaInP and c-Si under AM1.5

Table 3: Calculated current densities, open circuit voltage, fill factor and power conversion efficiency for each of the sub-cells and for the full cell of new model

Solar cell	Jsc (mA/cm ²)	Voc (V)	FF	η (%)
c-Si	9.2	0.6	83	6.4
GaInP	9.2	1.8	89	21.2
Series connection model (GaInP with c-Si)	9.2	2.4	94	28.0

Back-Connected (BJBC) c-Si bottom cell (Essig *et al.*, 2015). The structure of this experimental model is shown in Fig. 8.

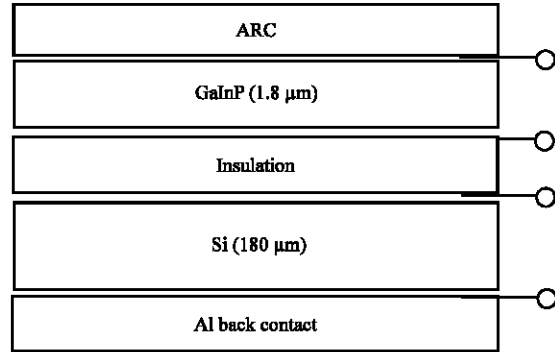


Fig. 8: Structure of the simplified GaInP on Si tandem solar cell being investigated with 4T configuration

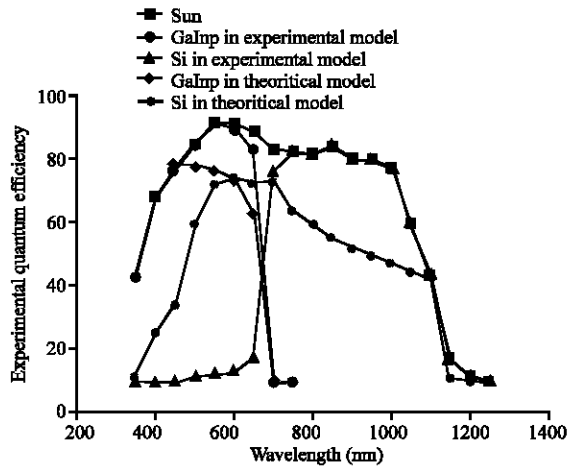


Fig. 9: The comparison between experimental and theoretical external quantum efficiency of tandem solar cell GaInP/c-Si

Table 4: Calculated current densities, open circuit voltage, fill factor and power conversion efficiency for each of the sub-cells and for the full cell of new model compared to the experimental model

Solar cell	Jsc (mA/cm ²)	Voc (V)	FF	η (%)
c-Si (theoretical)	9.2	0.6	83.0	6.40
GaInP(theoretical)	9.2	1.8	89.0	21.20
Series connection model (GaInP with c-Si) (theoretical)	9.2	2.4	94.0	28.00
c-Si (experimental)	23.3	0.605	60.5	8.54
GaInP (experimental)	14.6	1.44	87.9	18.54
Total of experimental model				27.0

RESULTS AND DISCUSSION

To compare the two models we prepare the curve of each in the same axis. Figure 9 and 10 show the external quantum efficiency and the curve I-V of the two models. Result of comparison is given in Table 4.

Higher efficiencies can be achieved with our theoretical tandem solar cell model. The experimental

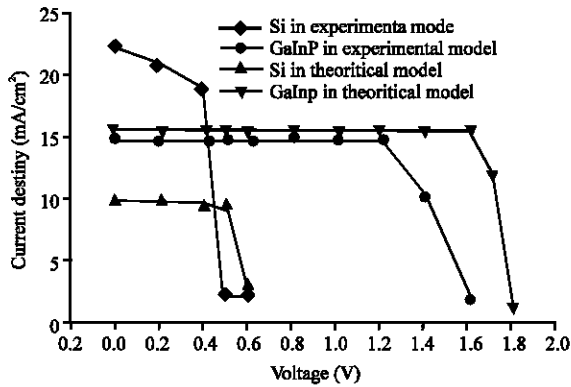


Fig. 10: The comparison between experimental and theoretical curve I-V of tandem solar cell GaInP/c-Si

model suffers from a low fill factor of 60.5% (for the bottom cell) caused by damage induced during the processing of the top cell and series resistances losses, this problem is resolved in our theoretical model by no connection directly between Si and GaInP. So, we arrived to a fill factor >80%.

CONCLUSION

The experimental model shows that mechanically stacked GaInP/c-Si tandem solar reached an efficiency of 27%. Whereas with our new structure we show that, we can arrived to efficiency greater than 27 % and with less cost of fabrication and less problem of coherence between materials. So, we can say that this theoretical model is an innovation in the field of tandem solar cells Si/III-V materials.

REFERENCES

- Cotal, H., C. Fetzer, J. Boisvert, G. Kinsey and R. King *et al.*, 2009. III-V multijunction solar cells for concentrating photovoltaics. *Energy Environ. Sci.*, 2: 174-192.
- Essig, S., S. Ward, M.A. Steiner, D.J. Friedman and J.F. Geisz *et al.*, 2015. Progress towards a 30% efficient GaInP-Si tandem solar cell. *Energy Procedia*, 77: 464-469.
- Fahrenbruch, A.L. and R.H. Bube, 1983. *Fundamentals of Solar Cells Photovoltaic Solar Energy Conversion*. Academic Press, New York, USA.,.
- Green, M.A., E.C. Cho, Y. Cho, E. Pink and T. Trupke *et al.*, 2005. All-silicon tandem cells based on artificial semiconductor synthesised using silicon quantum dots in a dielectric matrix. *Proceedings of the 20th Conference on European Photovoltaic Solar Energy*, June 6-10, 2005, Barcelona International Convention Centre, Barcelona, Spain, pp: 6-10.
- Guijiang, L., W. Jyhchiarnng and H. Meichun, 2010. Theoretical modeling of the interface recombination effect on the performance of III-V tandem solar cells. *J. Semicond.*, Vol. 31,
- Luque, A. and S. Hegedus, 2011. *Handbook of Photovoltaic Science and Engineering*. John Wiley & Sons, Hoboken, New Jersey, USA., ISBN:s9780470721698, Pages:1132.
- Petibon, S., 2009. [New distributed energy management and conversion architectures for photovoltaic applications]. Ph.D Thesis, Paul Sabatier University, Toulouse, France. (In French)
- Wurfel, P., 2005. *Physics of Solar Cells: From Principles to New Concepts*. Wiley-VCH, Berlin, Germany.,
- Yamaguchi, M., 2003. III-V compound multi-junction solar cells: Present and future. *Solar Energy Mater. Solar Cells*, 75: 261-269.